DOI: 10.1002/ejic.200500985

Syntheses, Structures, and Characterization of Two Manganese(II)-Aminobenzoic Complexes

Ruihu Wang,[a] Daqiang Yuan,[a] Feilong Jiang,[a] Lei Han,[a] Song Gao,[b] and Maochun Hong*[a]

Keywords: Manganese / Aminobenzoic acid / Magnetic properties

A discrete tetranuclear manganese(II) complex, $\{(H_3O)_2Mn_4(4\text{-Haba})_2(4\text{-aba})_6(SCN)_4(H_2O)_2\}$ (**1**) and a two-dimensional coordination polymer $[Mn(3\text{-aba})_2]_n$ (**2**) (4-Haba = 4-aminobenzoic acid, 3-Haba = 3-aminobenzoic acid), have been synthesized and characterized by elemental analyses, IR, X-ray crystallography, and magnetic susceptibility. In complex **1**, 4-aba in three types of coordination modes connects Mn^{II} centers to form a discrete tetranuclear anionic molecule. Hydrogen bonding interaction links the tetranuclear units to generate a one-dimensional supramolecular chain. In complex **2**, 3-aba in an *exo*-tridentate mode bridges six-coordinate Mn^{II} centers forming a two-dimensional coordination architecture. Studies of the magnetic susceptibilities of **1** and **2** reveal weak antiferromagnetic exchange interactions between adjacent Mn^{II} centers.

Introduction

A significant amount of research has been dedicated to the study of the magnetic behavior of discrete polynuclear entities and molecule-based coordination polymers with extended structures.[1–3] The increasing interest in this field is justified not only by the intellectual challenge of understanding the fundamental relationship between structures and magnetic properties, but also by the development of new types of functional molecule-based magnetic materials.[4–7] In this context, one of the points to be seriously considered for the preparation of these magnetic solids is the choice of appropriate bridging ligands, since they mediate superexchange interactions between the paramagnetic metal centers. The type, size, shape, flexibility, conformation, and symmetry of the ligands along with their connective patterns are all important parameters, affecting the type and magnitude of the magnetic exchange interaction.[5–8] In the course of formation of desirable magnetic complexes, certain features of the organic ligands connecting paramagnetic metal centers can be utilized and tuned. For example, the carboxyl group can not only bridge two or more metal centers to produce a wide variety of complexes ranging from zero-dimensional discrete molecules to three-dimensional architectures, but also can adopt various types of bridging conformation modes, such as the so-called *syn-syn*, *syn-anti*, and *anti-anti* modes (Scheme 4). The magnetic properties are closely related to the bridging modes adopted by the carboxyl group in these complexes.[9,10] Thus, in terms of constructing the extended structural motifs, either di- and muti-carboxyl ligands, or multifunctional carboxyl-containing ligands incorporating other coordination groups, such as N, and S, have been employed;[5,11,12] the N or S donor atoms coordinating to metal centers can result in fascinating extended complexes with beautiful aesthetics and useful functional properties.[13,14c] However, owing to the presence of many subtle factors in the assembly process and the difficulty in predicting the final architectures, the rational design of coordination complexes from multifunctional organic ligands and metal ions is still a challenge to chemists, and a great deal of work is required to extend the knowledge of relevant magnetic solids and establish proper synthetic strategies leading to desirable architectures and useful properties.

As a part of our work towards rational design and preparation of functional supramolecular complexes with intriguing structures and potential applications in optics, electrical conductivity, magnetism, and host-guest chemistry,[14,15] we have successfully prepared a series of Cd^{II} and Ag^{I} complexes from the multifunctional organic ligands 4-aminobenzoic acid (4-Haba) and 3-aminobenzoic acid (3-Haba) through combination of their amino and carboxyl groups.[15b,15c] It is known that high-spin manganese(II) contains five unpaired electrons and is quite oxophilic, and

[a] State Key Laboratory of Structural Chemistry, Fujian Institute of the Research on the Structure of Matter, Chinese Academy of Sciences,
Fuzhou, Fujian, 350002, China
Fax: +86-591-8371-4946
E-mail: hmc@ms.fjirsm.ac.cn
[b] State Key Laboratory of Rare Materials Chemistry and Applications, College of Chemistry and Molecular Engineering, Peking University,
Beijing, 100871, China

Supporting information for this article is available on the WWW under http://www.eurjic.org or from the author.

that the assembly of manganese(II) with organic ligands containing the carboxyl group is inclined to the formation of larger clusters and extended solids.[16] Moreover, carboxyl-bridged manganese(II) complexes have been known to exist at the active centers of some Mn^{II}-containing enzymes.[17] Recently, we have reported a three-dimensional manganese(II) complex from 4-Haba exhibiting ferrimagnetic and metamagnetic behavior.[15a] Considering the versatile bridging modes of the carboxyl group and efficient mediation of magnetic coupling in 4-aba and 3-aba, herein, we wish to report the syntheses and characterization of a discrete tetranuclear manganese(II) complex $\{(H_3O)_2[Mn_4(4\text{-Haba})_2(4\text{-aba})_6(SCN)_4(H_2O)_2]\}$ (**1**) and a two-dimensional coordination architecture $[Mn(3\text{-aba})_2]_n$ (**2**).

Result and Discussion

Synthesis and Characterization

Reaction of $MnCl_2{\cdot}4H_2O$, 4-Haba, and NaN_3 at room temperature produced a three-dimensional complex $[Mn_3(4\text{-aba})_6]_n$ (**3**),[15a] in which N_3^- is not involved in coordination to the Mn^{II} ion and acts as a base to deprotonate 4-Haba. Previous research demonstrates that the assembly process of 4-Haba and transitional metal ions has been highly influenced by counter anions, pH value, solvent system, and metal-to-ligand ratio besides the coordination nature of the metal ions.[15,18] In some cases, a subtle alteration in any of these factors can result in new complexes with different structural topologies and different functions. The successful isolation of **3** prompted us to prepare other Mn^{II} complexes from 4-Haba and 3-Haba through altering reaction-influencing factors. Instead of N_3^-, the use of SCN^- in the presence of NaOH led to a tetranuclear Mn^{II} complex (**1**), and the reaction of 3-Haba and $MnCl_2{\cdot}4H_2O$ in the presence of either NaN_3 or NH_4SCN and NaOH afforded the complex **2**. In the preparation of compounds **1**–**3**, the counter anions obviously have an important effect on their assembly process even if they are not present in the complexes. We presume that these counter anions coordinate to a part of the metal ions in solution and remain soluble species, whereas only the insoluble crystalline material can be isolated and identified. It is possible therefore, that the presence of these counter anions is important for the equilibrium that leads eventually to the isolation of the polynuclear carboxylates. It is well known that the relative orientation of the coordination sites in organic ligands is also one of the most important factors in controlling the construction of supramolecular architectures.[19] The assembly of organic ligands with different orientations of coordination sites and metal ions can produce different structural frameworks. Thus, the difference between complex **2** and complex **1** and **3** can be ascribed to the different stereochemistry of the ligands.

The C≡N stretching vibration of the thiocyanate group in **1** appears as a single strong peak at 2085 cm^{-1}, which is consistent with the occurrence of thiocyanate-N coordination.[20] The characteristic bands of the carboxyl group of 4-aba are shown at 1608 cm^{-1} for antisymmetric stretching and at 1406 and 1396 cm^{-1} for symmetric stretching. The separations (Δ) between ν_{asym}(–COO) and ν_{sym}(–COO) are 202 and 212 cm^{-1}, respectively, revealing that the carboxyl group of 4-aba functions in different bridging modes. The IR spectrum of complex **2** shows typical antisymmetric and symmetric stretching bands of the carboxyl group at 1579 and 1394 cm^{-1}, respectively, the Δ value is 185 cm^{-1}.

Structural Description

$\{(H_3O)_2[Mn_4(4\text{-Haba})_2(4\text{-aba})_6(SCN)_4(H_2O)_2]\}$ (1): Single-crystal X-ray diffraction analysis reveals that **1** consists of a tetranuclear $[Mn_4(4\text{-Haba})_2(4\text{-aba})_6(SCN)_4(H_2O)_2]^{2-}$ anion and two lattice water molecules; the two lattice water molecules or two of the total eight amino groups of the tetranuclear unit are required to be protonated to achieve overall charge balance. These protons were not located crystallographically and could reside on any of the eight amino groups or two lattice water molecules. Since the amino group is more basic than the water molecule, the protonation likely occurs at the amino groups of some ligands. As shown in Figure 1 (a), there are two crystallographically independent Mn^{II} centers in the tetranuclear anionic framework. Mn(1) is coordinated by two carboxyl oxygen atoms and one chelating carboxyl group from three different 4-aba, one water molecule, and one nitrogen atom of the terminal SCN^-. However, Mn(2) is coordinated by four carboxyl oxygen atoms from different 4-aba, one carboxyl oxygen atom from 4-Haba, and one nitrogen atom of the terminal SCN^-. Thus, Mn(1) and Mn(2) are in a highly distorted octahedral geometry. Mn(1)–O(21)–Mn(2) and Mn(1)–O(41)–Mn(2) bond angles are 94.30(14) and 98.59(15)°, respectively. The SCN^- groups are almost linear with the N(1)–C(1)–S(1) and N(2)–C(2)–S(2) bond angles being 177.8(6) and 179.0(8)°, respectively. The connections between Mn^{II} and SCN^- groups are slightly bent with the C(1)–N(1)–Mn(2) and C(2)–N(2)–Mn(1) bond angles being 151.5(5) and 168.4(6)°, respectively. 4-Haba acts as a monodentate ligand through one carboxylic oxygen atom coordinating to Mn(2) (Scheme 1, a). However, 4-aba has three distinctly different coordination modes, in which the amino nitrogen atom is not involved in coordination with Mn^{II}: one behaves in a μ_2-η^2-carboxyl bridging mode (Scheme 1, b); the second adopts a μ_2-chelating/bridging mode (Scheme 1, c); and the third acts as a μ_3-carboxyl bridge (Scheme 1, d). Thus, Mn(1) and Mn(2) are linked together by three different types of 4-aba through one *syn-syn* μ-carboxyl bridge (Scheme 1, b), two μ-O atoms from the μ_2-chelating/bridging carboxyl group (Scheme 1, c), and the μ_3-carboxyl group (Scheme 1, d), respectively. The separation of Mn(1)···Mn(2) is 3.407 Å. A similar molecular geometry to this kind of connection has been found in $[Mn_3(HCOO)_6]$, where the Mn–Mn connectivity is 3.625 Å.[21] The other oxygen atom in the μ_3-carboxyl group of 4-aba (Scheme 1, d) coordinates to Mn(2) and further links the two independent Mn^{II} into a tetranuclear Mn^{II}

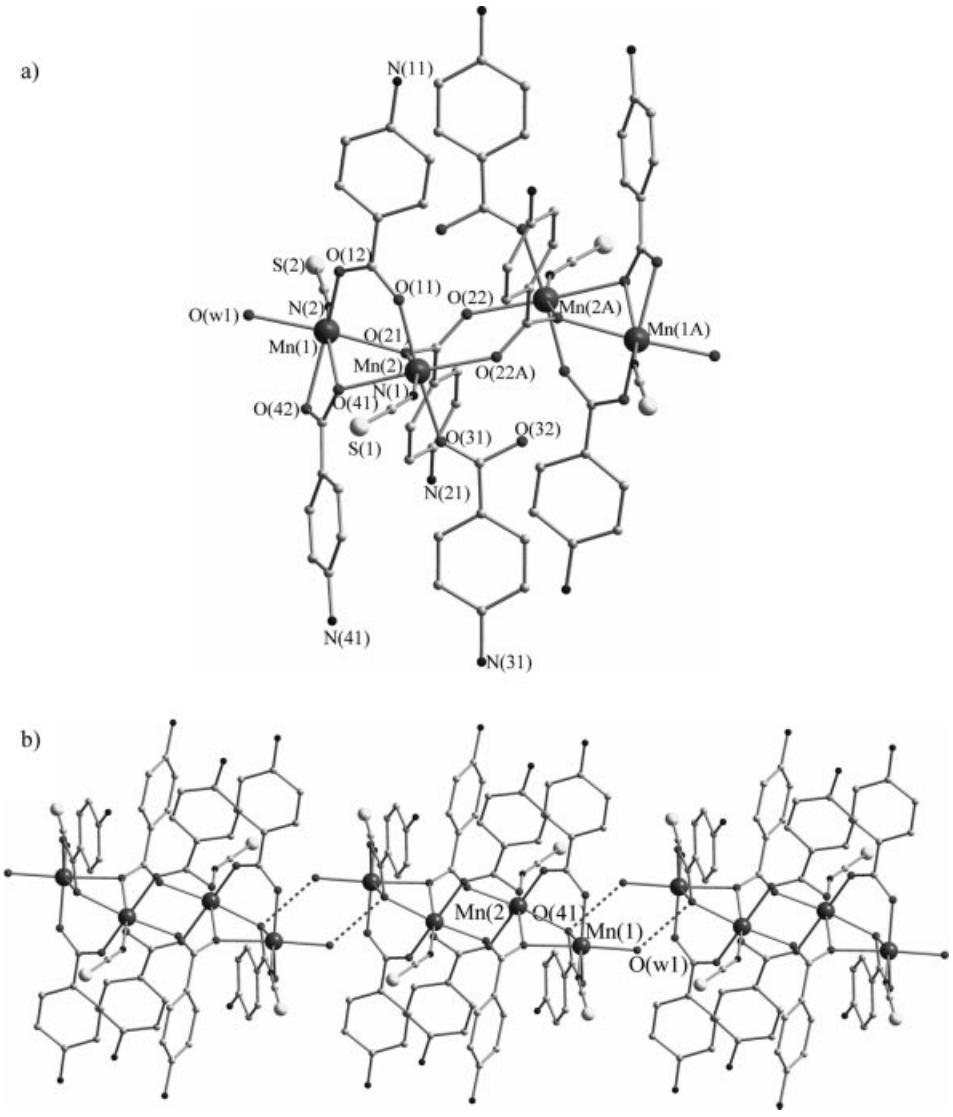

Figure 1. (a) View of the tetranuclear Mn^{II} anionic framework in **1**. (A) $2 - x$, $1 - y$, $1 - z$. (b) View of a one-dimensional hydrogen bonding chain consisting of tetranuclear Mn^{II} anions in **1**.

cluster, in which the Mn(2)···Mn(2A) and Mn(1)···Mn(2A) separations bridged by the carboxyl group of 4-aba are 5.058 and 6.150 Å, respectively. The topology of the rhombic tetranuclear Mn^{II} cluster is rather unusual, and it has an unprecedented $[Mn_4(\mu_3\text{-4-aba})_2(\mu_2\text{-}\eta^2\text{-4-aba})_2]$ core, which is different to several rhombic or butterfly-like tetranuclear Mn clusters with an $[Mn_4(\mu\text{-carboxylic})]$ or $[Mn_4(\mu_3\text{-phth})_2]$ core that have been reported.[22] The hydrogen bonding interaction between the coordinated water molecule and the μ-O atom in the μ_3-carboxyl of 4-aba [OW1–H(1)···O(41)^i 2.854(7) Å; symmetry code (i) $-x + 1$, $-y + 1$, $-z + 1$] cross-links the tetramers into a one-dimensional supramolecular chain. The closest Mn···Mn distance between adjacent tetramers in the chain is 4.994 Å (Figure 1, b).

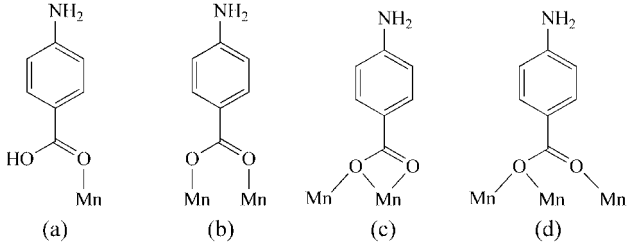

Scheme 1. Coordination modes of 4-Haba and 4-aba in **1**.

$[Mn(3\text{-aba})_2]_n$ (2): Complex **2** is a two-dimensional coordination polymer based on infinite Mn–O–C–O chains. As shown in Figure 2 (a), Mn(1) is in a slightly distorted octahedral coordination environment and is coordinated by four carboxyl oxygen atoms and two nitrogen atoms from six different 3-aba. Four carboxyl oxygen atoms comprise the equatorial plane and Mn^{II} is coplanar with the mean plane of four equatorial carboxyl oxygen atoms, and the two amino nitrogen atoms occupy the axial positions. The bond angles between the *cis* donors around Mn^{II} range from

85.27(17) to 94.73(17)°. The Mn–N bond length of 2.290(5) Å is slightly longer then the Mn–O bond lengths of 2.150(4) and 2.201(4) Å, suggesting an elongated octahedron. In addition, 3-aba acts as an *exo*-tridentate bridge through the amino nitrogen atom and μ_2-η^2-carboxyl group (Scheme 2). The carboxyl group is slightly distorted with respect to the phenyl ring with the dihedral angle between them being 11.8°. The double *syn-syn* mode $\mu_{1,3}$-carboxyl bridges coming from two different 3-aba ligands exist between neighboring Mn^{II} ions forming an infinite Mn–O–C–O chain with the C–O–Mn bond angles being 124.6(3) and 133.8(3)°. The closest Mn···Mn distance within the chain is 4.607 Å. As shown in Figure 2 (b), the chains are cross-linked into a two-dimensional layer structure through the amino nitrogen atom of 3-aba coordinating to the remaining coordination sites of Mn^{II}. The shortest inter-chain Mn···Mn distance is 8.129 Å. There are no other short contacts or noteworthy aryl-aryl interactions between the adjacent two-dimensional layers.

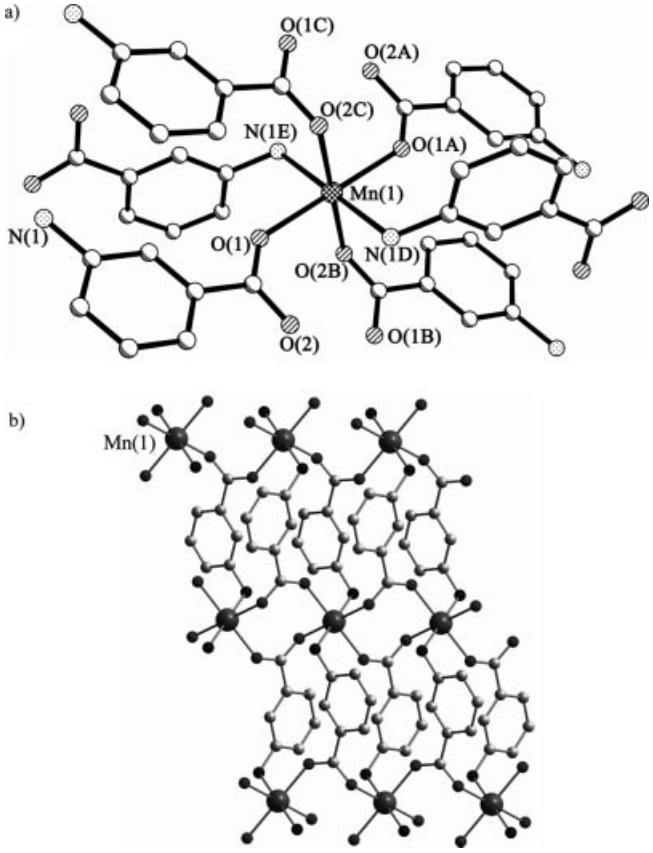

Figure 2. (a) View of the coordination environment around Mn^{II} in **2**. (A) 1 – *x*, –*y*, 1 – *z*; (B) 1 – *x*, –*y* – 1, 1 – *z*; (C) *x*, 1 + *y*, *z*; (D) *x* – 1/2, –*y* – 1/2, *z* – 1/2; (E) 3/2 – *x*, 1/2 + *y*, 3/2 – *z*. (b) View of a pack diagram along the *a* axis showing the two-dimensional network in **2**.

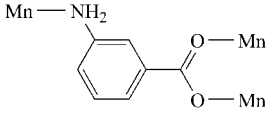

Scheme 2. Coordination mode of 3-aba in **2**.

Magnetic Properties

The magnetic susceptibilities of complexes **1** and **2** were measured in the 2–300 K temperature range and are shown in Figure 3 and Figure 4, respectively. The experimental $\chi_m T$ values of **1** and **2** at room temperature are 4.66 and 4.24 $cm^3 \cdot mol^{-1} \cdot K$ per Mn^{II}, respectively, close to the spin-only value expected for an uncoupled high-spin Mn^{II} ion (4.38 $cm^3 \cdot mol^{-1} \cdot K$). As the temperature is lowered to 2 K, the $\chi_m T$ products decrease first slowly and then rapidly. The behavior suggests that antiferromagnetic interactions are operative in the two complexes. The temperature dependence of the reciprocal susceptibilities ($1/\chi_m$) obeys the Curie–Weiss law above 5 K for **1** and 15 K for **2** with θ = –8.9 and –13.9 K for **1** and **2**, respectively. The negative θ values support the presence of overall antiferromagnetic interactions in the two complexes.

The crystallographic data of **1** suggest that there are three different types of superexchange pathways within the tetranuclear unit, which can be schematized as shown in Scheme 3. Therefore, the magnetic data of **1** should be analyzed by an analytical expression based on the Hamiltonian in Equation (1).

$$H = -2J_1S_1S_2 - 2J_2(S_1S_3 + S_2S_4) - 2J_3(S_1S_4 + S_2S_3) \quad (1)$$

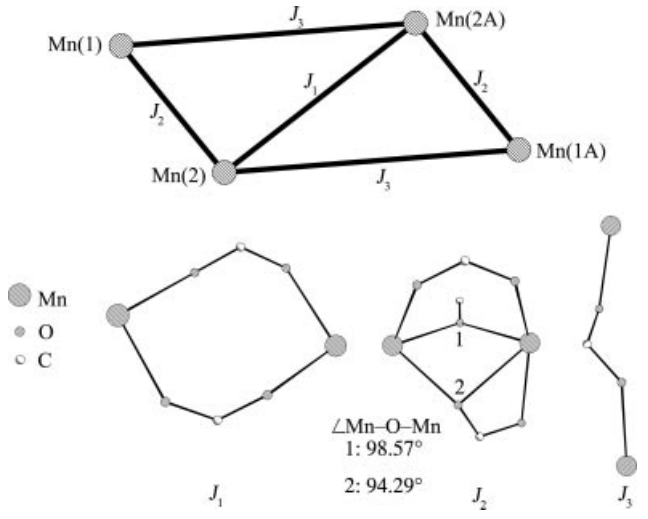

Scheme 3. Spin topology for **1** assuming three different *J* values.

Calculations were performed with the magnetism package MAGPACK.[23] The best-fit parameters obtained were J_1 = –1.84(1) cm^{-1}, J_2 = –0.18(2) cm^{-1}, J_3 = 0.02(1) cm^{-1}, g = 2.090(2) and $R = 2.6 \cdot 10^{-4}$ ($R = \Sigma[(\chi_m T)_{obs}^2 - (\chi_m T)_{calc}^2]/\Sigma[(\chi_m T)_{obs}^2]$). As expected from the structural parameters depicted in Scheme 3, the results show the presence of two antiferromagnetic and one very weak ferromagnetic interaction. The difference in the magnetic exchange interactions found for **1** can be satisfactorily explained in terms of the conformation modes of the carboxyl bridge. The exchange

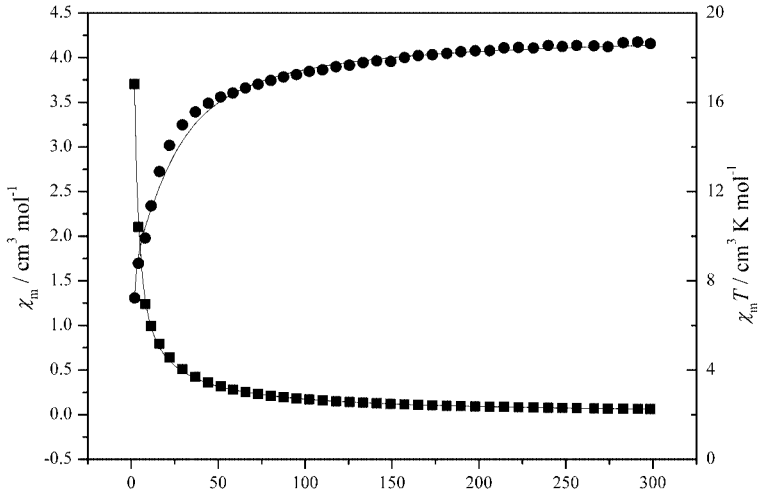

Figure 3. Temperature dependence of χ_m (■) and $\chi_m T$ (●) values for complex **1**. The solid lines correspond to the best-fit curves using the parameters described in the text.

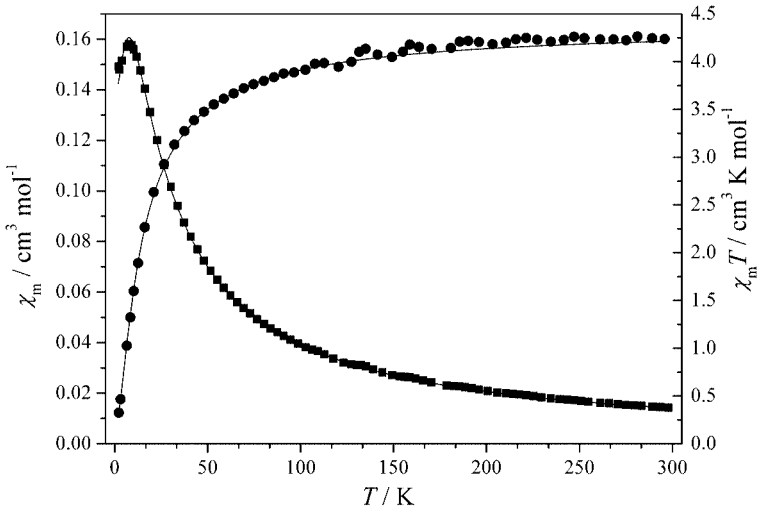

Figure 4. Temperature dependence of χ_m (■) and $\chi_m T$ (●) values for complex **2**. The solid lines correspond to the best-fit curves using the parameters described in the text.

coupling through the carboxyl bridge is highly dependent on the conformation modes (Scheme 4) of the bridge between the metal centers.[16b] The *syn-syn* mode provides small metal–metal distances and a good overlap of magnetic orbitals, which usually induces antiferromagnetic coupling in Mn^{II} polynuclear complexes.[24] The *syn-anti* mode induces much smaller J values because of the expanded metal center and a mismatch in the orientation of magnetic orbitals.[8b,9] The few examples involving the *anti-anti* mode indicated that this coupling is weakly ferromagnetic or antiferromagnetic.[9,25] Coupling J_1 arises from the double *syn-syn* carboxyl bridge and gives a weak antiferromagnetic coupling in this case, but coupling J_3 through the single *anti-anti* carboxyl bridge gives very weak ferromagnetic coupling. The J_1 value is larger than the J_3 value, which shows that the *syn-syn* carboxyl bridge is more favorable than the *anti-anti* mode for transmission of the magnetic coupling interaction.[9,26] In the coupling J_2, the effect of the two carboxyl bridges in *syn-syn* and *syn-anti* configuration is antiferromagnetic, but the two μ–O bridges with Mn–O–Mn angles of 98.59° and 94.30° may show weak ferromagnetic coupling and will reduce the antiferromagnetic contribution.[27]

The situation for **2** is much simpler. Magnetically, **2** is a uniform chain, in which there is only one type of superexchange pathway: the double *syn-syn* mode carboxyl bridge. The interchain magnetic interactions should be much weaker. The magnetic interaction within the chain can be expressed by the isotropic Hamiltonian $H = -2J\Sigma S_i S_{i+1}$, where J is the coupling constant between neighboring metal ions. To simulate the experimental magnetic behavior, we used the analytical expression derived by Fisher[28] for a one-dimensional Heisenberg chain of classical spins [$S = 5/2$, Equation (2)].

$$\chi_{chain} = [Ng^2\beta^2 S(S + 1)/(3kT)][(1 + u)/(1 - u)] \quad (2)$$

where N is Avogadro's number, β is Bohr's magneton, k is Boltzmann's constant, and u is the well-known Langevin

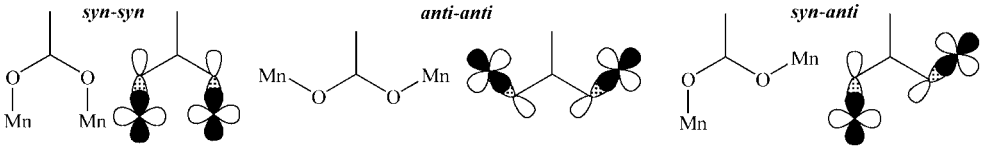

Scheme 4. Schematic representations of the coordination modes for the carboxylate bridges and the overlap of *d-p* magnetic orbitals.

function: $u = \coth[2JS(S + 1)/kT] - kT/[2JS(S + 1)]$. To take into account the interchain interaction, we applied the molecular field approximation [Equation (3)].[29]

$$\chi = \chi_{chain}/[1 - (2zJ'/Ng^2\beta^2)\chi_{chain}] \quad (3)$$

The best least-squares fit of the theoretical equation to experimental data leads to $J = -0.640(3)\ cm^{-1}$, $2zJ' = 0.070(1)\ cm^{-1}$, and $g = 2.000(2)$. The J value suggests that a weak antiferromagnetic interaction between neighboring Mn^{II} ions is mediated through the double *syn-syn* mode μ_2-carboxyl bridges. It is comparable to those reported for other Mn^{II} species with similar double carboxyl bridges.[16c]

Conclusions

One tetranuclear manganese(II) complex and one two-dimensional coordination polymer based on infinite Mn–O–C–O chains from 4-Haba and 3-Haba, respectively, have been synthesized and characterized crystallographically and magnetically. The structural difference between **1** and **2** is ascribed to the relatively different orientation of coordination sites of 4-aba and 3-aba. The analysis of the magnetic properties of **1** and **2** suggests weak antiferromagnetic interactions. Three types of magnetic interaction operative in complex **1** result in an overall antiferromagnetic behavior, as indicated by the temperature dependence of the magnetic susceptibility. Complex **2** exhibits weak antiferromagnetic interactions through double μ_2-η^2-carboxyl bridges within the chain.

Experimental Section

General: All reagents were commercially available and used as purchased. The IR spectra (KBr disk) were recorded with a Magna 750 FT-IR spectrophotometer. C, H, and N elemental analyses were determined with an Elementary Vario ELIII elemental analyzer. Variable-temperature magnetic susceptibilities were measured with a Quantum Design MPMS SQUID magnetometer equipped with a 5 kOe magnet in the temperature range 2–300 K. The observed susceptibility data were corrected for underlying diamagnetism by using Pascal's constants.[1b]

Synthesis of $\{(H_3O)_2[Mn_4(4\text{-Haba})_2(4\text{-aba})_6(SCN)_4(H_2O)_2]\}$ (1): A solution of $MnCl_2{\cdot}4H_2O$ (0.10 g, 0.5 mmol) and NH_4SCN (0.08 g, 1.0 mmol) in H_2O (10 mL) was added slowly to a solution of 4-aminobenzoic acid (0.07 g, 0.5 mmol) in ethanol (10 mL) under stirring, then 0.1 mol·L^{-1} NaOH aqueous solution was added dropwise to the reaction mixture until a small amount of precipitate was formed (pH = 4.0–4.5). The precipitate was filtered off and the filtrate was allowed to stand at room temperature for about 2 weeks, yellow crystals were produced. Yield: 0.13 g (61%). $C_{30}H_{30}Mn_2N_6O_{10}S_2$ (808.60): calcd. C 44.56, H 3.71, N 10.39; found C 44.51, H 3.67, N 10.35. IR (KBr): $\tilde{\nu}$ = 3460 (w), 3365 (s), 3271 (m), 2085 (s), 1608 (s), 1574 (w), 1528 (s), 1508 (s), 1406 (vs), 1396 (vs), 1327 (w), 1292 (w), 1261 (w), 1184 (w), 1174 (w), 1128 (vw), 1093 (vw), 1014 (vw), 978 (w), 957 (vw), 850 (vw), 789 (m), 700 (vw), 621 (w), 552 (vw), 492 (vw) cm^{-1}.

Synthesis of $[Mn(3\text{-aba})_2]_n$ (2): The procedure is similar to the synthesis of **1** except that 3-aminobenzoic acid (0.07 g, 0.5 mmol) was used instead of 4-aminobenzoic acid. Yield: 0.09 g (55%). $C_{14}H_{12}MnN_2O_4$ (327.2): calcd. C 51.39, H 3.67, N 8.56; found C 51.35, H 3.61, N 8.53. IR (KBr): $\tilde{\nu}$ = 3358 (m), 3284 (w), 1579 (m), 1547 (s), 1454 (m), 1394 (s), 1311 (vw), 1246 (w), 1120 (vw), 1074 (vw), 976 (m), 924 (w), 912 (w), 901 (w), 787 (m), 775 (s), 690 (vw), 669 (vw), 565 (vw), 546 (vw), 517 (vw) cm^{-1}. Compound **2** can also be obtained through the directed reaction of 3-Haba, $MnCl_2{\cdot}4H_2O$, and NaN_3 in EtOH/H_2O at room temperature.

Table 1. Selected bond lengths [Å] and angles [°] for **1** and **2**.

Complex **1**			
Mn(1)–O(12)	2.093(4)	Mn(1)–N(2)	2.122(7)
Mn(1)–O(W1)	2.184(4)	Mn(1)–O(42)	2.220(4)
Mn(1)–O(21)	2.257(4)	Mn(1)–O(41)	2.401(4)
Mn(2)–O(11)	2.095(4)	Mn(2)–N(1)	2.164(6)
Mn(2)–O(31)	2.186(4)	Mn(2)–O(22A)	2.198(4)
Mn(2)–O(21)	2.238(4)	Mn(2)–O(41)	2.244(4)
O(12)–Mn(1)–N(2)	108.2(2)	O(12)–Mn(1)–O(W1)	89.28(17)
N(2)–Mn(1)–OW1	89.6(2)	O(12)–Mn(1)–O(42)	148.26(18)
N(2)–Mn(1)–O(42)	103.4(2)	O(W1)–Mn(1)–O(42)	87.34(18)
O(12)–Mn(1)–O(21)	94.53(16)	N(2)–Mn(1)–O(21)	90.4(2)
O(W1)–Mn(1)–O(21)	176.00(17)	O(42)–Mn(1)–O(21)	88.78(15)
O(12)–Mn(1)–O(41)	93.94(16)	N(2)–Mn(1)–O(41)	154.1(2)
O(W1)–Mn(1)–O(41)	104.41(17)	O(42)–Mn(1)–O(41)	56.64(15)
O(21)–Mn(1)–O(41)	74.16(14)	O(11)–Mn(2)–N(1)	92.83(19)
O(11)–Mn(2)–O(31)	171.89(18)	N(1)–Mn(2)–O(31)	94.87(19)
O(11)–Mn(2)–O(22A)	93.59(16)	N(1)–Mn(2)–O(22A)	94.5(2)
O(31)–Mn(2)–O(22A)	83.31(16)	O(11)–Mn(2)–O(21)	89.19(16)
N(1)–Mn(2)–O(21)	167.71(19)	O(31)–Mn(2)–O(21)	83.81(16)
O(22A)–Mn(2)–O(21)	97.51(16)	O(11)–Mn(2)–O(41)	90.35(16)
N(1)–Mn(2)–O(41)	90.17(19)	O(31)–Mn(2)–O(41)	92.14(15)
O(22A)–Mn(2)–O(41)	173.76(16)	O(21)–Mn(2)–O(41)	77.69(15)
Complex **2**			
Mn–O(1)	2.150(4)	Mn–O(2B)	2.201(4)
Mn–N(1D)	2.290(5)		
O(1)–Mn–O(2C)	88.94(15)	O(1)–Mn–O(2B)	91.06(15)
O(1)–Mn–N(1D)	90.41(16)	O(1A)–Mn–O(2C)	91.06(15)
O(2C)–Mn–N(1D)	94.73(17)	O(2B)–Mn–N(1D)	85.27(17)
O(1A)–Mn–N(1E)	90.41(16)	O(1)–Mn–N(1E)	89.59(16)
O(2C)–Mn–N(1E)	85.27(17)	O(2B)–Mn–N(1E)	94.73(17)

Symmetry code: **1** (A) $-x + 2, -y + 1, -z + 1$; **2** (A) $-x + 1, -y, -z + 1$; (B) $-x + 1, -y - 1, -z + 1$; (C) $x, y + 1, z$; (D) $x - 1/2, -y - 1/2, z - 1/2$; (E) $-x + 3/2, y + 1/2, -z + 3/2$

X-ray Crystallography: Intensity data for **1** and **2** were measured with a Siemens Smart CCD diffractometer with graphite-monochromated Mo-K_α radiation (λ = 0.71073 Å) at room temperature. All empirical absorption corrections were applied using the SADABS program.[30] The structures were solved by direct methods[31] and refined on F^2 by full-matrix least-squares using the SHELXL-97 program package.[32] The positions of H atoms were generated geometrically (C–H bond fixed at 0.96 Å), assigned isotropic thermal parameters, and allowed to ride on their parent carbon atoms before the final cycle of refinement. No attempt was made to locate the hydrogen atoms of water. The selected bond lengths and angles for **1** and **2** are listed in Table 1.

Crystal Data for 1: $C_{30}H_{30}Mn_2N_6O_{10}S_2$, Mr = 808.60, 0.46 × 0.34 × 0.26 mm, triclinic, space group $P\bar{1}$ (No. 2), a = 12.2553(2), b = 12.28000(10), c = 12.2833(2) Å, α = 80.774(1), β = 85.798(1), γ = 67.587(1)°, V = 1686.68(4) Å^3, Z = 2, D_c = 1.592 g/cm^3, F(000) = 828, Mo-K_α radiation, λ = 0.71073 Å, T = 173(2) K, $2\theta_{max}$ = 50.1°, 8783 reflections collected, 5900 unique (R_{int} = 0.0320). Final $GooF$ = 1.088, $R1$ = 0.0738, $wR2$ = 0.1414, R indices based on 4667 reflections with $I > 2\sigma(I)$ (refinement on F^2), 455 parameters, μ = 0.938 mm^{-1}.

Crystal Data for 2: $C_{14}H_{12}MnN_2O_4$, Mr = 327.20, 0.30 × 0.26 × 0.20 mm, monoclinic, space group $P2_1/n$ (No. 14), a = 8.8522(17), b = 4.6071(9), c = 15.377(3) Å, β = 105.279(3)°, V = 604.9(2) Å^3, Z = 2, D_c = 1.796 g/cm^3, F(000) = 334, Mo-K_α radiation, λ = 0.71073 Å, T = 293(2) K, $2\theta_{max}$ = 50.2°, 1785 reflections collected, 1054 unique (R_{int} = 0.0400). Final $GooF$ = 1.247, $R1$ = 0.0603, $wR2$ = 0.1243, R indices based on 866 reflections with $I > 2\sigma(I)$ (refinement on F^2), 121 parameters, μ = 1.110 mm^{-1}.

CCDC-288647 and -288648 (for **1** and **2**) contain the supplementary crystallographic data for this paper. These data can be obtained free of charge from The Cambridge Crystallographic Data Centre via www.ccdc.cam.ac.uk/data_request/cif.

Supporting Information (for details see the footnote on the first page of this article): Figure S1, packing diagram of **1** along the c axis and Figure S2, packing diagram of **2** along the b axis.

Acknowledgments

This work was supported by the National Nature Science Foundation of China (No. 20231020) and Nature Science Foundation of Fujian Province.

[1] a) J. S. Miller, M. Drilon, *Magnetism: Molecules to Materials*, Wiley-VCH, Weinheim, **2002**, vol. 3; b) O. Kahn, *Molecular Magnetism*, VCH, Weinheim, **1993**.

[2] J. Ribas, A. Escuer, M. Monfort, R. Vicente, R. Cortes, L. Lezama, T. Rojo, *Coord. Chem. Rev.* **1999**, *195*, 1027–1068 and references therein.

[3] a) J. Larionova, R. Clerac, J. Sanchiz, O. Kahn, S. Golhen, L. Ouahab, *J. Am. Chem. Soc.* **1998**, *120*, 13088–13095; b) C. Boskovic, E. K. Brechin, W. E. Streib, K. Folting, D. N. Hendrickson, G. Christou, *Chem. Commun.* **2001**, 467–468.

[4] C. Janiak, *Dalton Trans.* **2003**, 2781–2804.

[5] a) K. Barthelet, J. Marrot, D. Riou, G. Ferey, *Angew. Chem. Int. Ed.* **2002**, *41*, 281–284; b) N. Guillou, S. Pastre, C. Livage, G. Ferey, *Chem. Commun.* **2002**, 2358–2359.

[6] a) E. Q. Gao, S. Q. Bai, Z. M. Wang, C. H. Yan, *J. Am. Chem. Soc.* **2003**, *125*, 4984–4985; b) M. Minguet, D. Luneau, E. Lhotel, V. Villar, C. Paulsen, D. B. Amabilino, J. Veciana, *Angew. Chem. Int. Ed.* **2002**, *41*, 586–589; c) B. O. Patrick, W. M. Reiff, V. Sanchez, A. Storr, R. C. Thompson, *Inorg. Chem.* **2004**, *43*, 2330–2339.

[7] a) J. R. Galan-Mascaros, K. R. Dunbar, *Angew. Chem. Int. Ed.* **2003**, *42*, 2289–2293; b) H. L. Sun, B. Q. Ma, S. Gao, G. Su, *Chem. Commun.* **2001**, 2586–2587; c) M. Kurmoo, H. Kumagai, M. A. Green, B. W. Lovett, S. J. Blundell, A. Ardavan, J. Singleton, *J. Solid State Chem.* **2001**, *159*, 343–351.

[8] a) K. Okada, O. Nagao, H. Mori, M. Kozaki, D. Shiomi, K. Sato, T. Takui, Y. Kitagawa, K. Yamaguchi, *Inorg. Chem.* **2003**, *42*, 3221–3228; b) C. Policar, F. Lambert, M. Cesario, I. Morgenstern-Badarau, *Eur. J. Inorg. Chem.* **1999**, 2201–2207.

[9] E. Colacio, J. M. Domínguez-Vera, M. Ghazi, R. Kivekäs, M. Klinga, J. M. Moreno, *Eur. J. Inorg. Chem.* **1999**, 441–445 and references cited therein.

[10] a) P. King, R. Clerac, C. E. Anson, C. Coulon, A. K. Powell, *Inorg. Chem.* **2003**, *42*, 3492–3500; b) D. Schulz, T. Weyhermüller, K. Wieghardt, C. Butzlaff, A. X. Trautwein, *Inorg. Chim. Acta* **1996**, *246*, 387–394.

[11] a) S. Konar, P. S. Mukherjee, E. Zangrando, F. Lloret, N. R. Chaudhuri, *Angew. Chem. Int. Ed.* **2002**, *41*, 1561–1563; b) H. J. Chen, Z. W. Mao, S. Gao, X. M. Chen, *Chem. Commun.* **2001**, 2320–2321.

[12] a) P. M. Forster, A. K. Cheetham, *Angew. Chem. Int. Ed.* **2002**, *41*, 457–459; b) Z. L. Huang, M. Drillon, N. Masciocchi, A. Sironi, J. T. Zhao, P. Rabu, P. Panissod, *Chem. Mater.* **2000**, *12*, 2805–2812; c) J. M. Rueff, S. Pillet, N. Claiser, G. Bonaventure, M. Souhassou, P. Rabu, *Eur. J. Inorg. Chem.* **2002**, 895–900.

[13] a) D. Cave, J. M. Gascon, A. D. Bond, S. J. Teat, P. T. Wood, *Chem. Commun.* **2002**, 1050–1051; b) W. B. Lin, O. R. Evans, G. T. Yee, *J. Solid State Chem.* **2000**, *152*, 152–158; c) S. M. Humphrey, R. A. Mole, J. M. Rawson, P. T. Wood, *Dalton Trans.* **2004**, 1670–1678.

[14] a) M. C. Hong, Y. J. Zhao, W. P. Su, R. Cao, M. Fujita, Z. Y. Zhou, A. S. C. Chan, *J. Am. Chem. Soc.* **2000**, *122*, 4819–4820; b) W. P. Su, M. C. Hong, J. B. Weng, R. Cao, S. F. Lu, *Angew. Chem. Int. Ed.* **2000**, *39*, 2911–2914; c) Y. J. Zhao, M. C. Hong, Y. C. Liang, R. Cao, W. J. Li, J. B. Weng, S. F. Lu, *Chem. Commun.* **2001**, 1020–1021.

[15] a) R. H. Wang, E. Q. Gao, M. C. Hong, S. Gao, J. H. Luo, Z. Z. Lin, L. Han, R. Cao, *Inorg. Chem.* **2003**, *42*, 5486–5488; b) R. H. Wang, M. C. Hong, J. H. Luo, R. Cao, Q. Shi, J. B. Weng, *Eur. J. Inorg. Chem.* **2002**, 2904–2912; c) R. H. Wang, M. C. Hong, J. H. Luo, F. L. Jiang, L. Han, Z. Z. Lin, R. Cao, *Inorg. Chim. Acta* **2004**, *357*, 103–114.

[16] a) J. D. Martin, R. F. Hess, *Chem. Commun.* **1996**, 2419–2420; b) T. K. Maji, S. Sain, G. Mostafa, T. H. Lu, J. Ribas, M. Monfort, N. R. Chaudhuri, *Inorg. Chem.* **2003**, *42*, 709–716; c) W. Chen, Q. Yue, C. Chen, H. M. Yuan, W. Xu, J. S. Chen, S. N. Wang, *Dalton Trans.* **2003**, 28–30; d) H. H. Zhao, C. P. Berlinguette, J. Bacsa, A. V. Prosvirin, J. K. Bera, S. E. Tichy, E. J. Schelter, K. R. Dunbar, *Inorg. Chem.* **2004**, *43*, 1359–1369.

[17] a) V. L. Pecoraro, *Manganese Redox Enzymes*, VCH, Weinheim, **1992**; b) R. L. Rardin, P. Poganiuch, A. Bino, D. P. Goldberg, W. B. Tolman, S. C. Liu, S. J. Lippard, *J. Am. Chem. Soc.* **1992**, *114*, 5240–5249; c) K. F. Hsu, S. L. Wang, *Inorg. Chem.* **2000**, *39*, 1773–1778.

[18] a) P. J. Smith, R. O. Day, V. Chandrasekhar, J. M. Holmes, R. Holmes, *Inorg. Chem.* **1986**, *25*, 2495–2499; b) L. P. Battaglia, A. C. Bonamartini, S. Ianelli, M. A. Zoroddu, G. Sanna, *J. Chem. Soc., Faraday Trans.* **1991**, *87*, 3863–3867; c) M. R. Sundberg, J. K. Koskimies, J. Matikainen, H. Tylli, *Inorg. Chim. Acta* **1998**, *268*, 21–30; d) H. J. Chen, X. M. Chen, *Inorg. Chim. Acta* **2002**, *329*, 13–21; e) G. Smith, K. A. Byriel, C. H. L. Kennard, *Aust. J. Chem.* **1999**, *52*, 325–327.

[19] Z. He, Z. M. Wang, C. H. Yan, *CrystEngComm* **2005**, *7*, 143–150.

[20] a) Q. H. Zhao, H. F. Li, X. F. Wang, Z. D. Chen, *New J. Chem.* **2002**, *26*, 1709–1710; b) G. A. Van Albada, R. C. Guijt, J. G. Haasnoot, M. Lutz, A. L. Spek, J. Reedijk, *Eur. J. Inorg. Chem.* **2000**, 121–126.

[21] a) Z. M. Wang, B. Zhang, H. Fujiwara, H. Kobayashi, M. Kurmoo, *Chem. Commun.* **2004**, 416–417; b) R. D. Poulsen, A.

Bentien, M. Chevalier, B. B. Iversen, *J. Am. Chem. Soc.* **2005**, *127*, 9156–9166.
[22] a) C. B. Ma, W. G. Wang, X. F. Zhang, C. N. Chen, Q. T. Liu, H. P. Zhu, D. Z. Liao, L. C. Li, *Eur. J. Inorg. Chem.* **2004**, 3522–3532; b) G. Aromi, S. M. J. Aubin, M. A. Bolcar, G. Christou, H. J. Eppley, K. Folting, D. N. Hendrickson, J. C. Huffman, R. C. Squire, H.-L. Tsai, S. Wang, M. W. Wemple, *Polyhedron* **1998**, *17*, 3005–3020; c) G. Aromi, M. W. Wemple, S. M. J. Aubin, K. Folting, D. N. Hendrickson, G. Christou, *J. Am. Chem. Soc.* **1998**, *120*, 5850–5851; d) R. J. Kulawiec, R. H. Crabtree, G. W. Brudvig, G. K. Schulte, *Inorg. Chem.* **1988**, *27*, 1309–1311; e) E. Libby, J. K. McCusker, E. A. Schmitt, K. Folting, D. N. Hendrickson, G. Christou, *Inorg. Chem.* **1991**, *30*, 3486–3495; f) S. Wang, K. Folting, W. E. Streib, E. A. Schmitt, J. K. McCusker, D. N. Hendrickson, G. Christou, *Angew. Chem. Int. Ed. Engl.* **1991**, *30*, 304–306.
[23] a) J. J. Borrás-Almenar, J. M. Clemente-Juan, E. Coronado, B. Tsukerblat, *Inorg. Chem.* **1999**, *38*, 6081–6088; b) J. J. Borrás-Almenar, J. M. Clemente-Juan, E. Coronado, B. S. Tsukerblat, *J. Comput. Chem.* **2001**, *22*, 985–991.
[24] X. S. Tan, D. F. Xiang, W. X. Tang, J. Sun, *Polyhedron* **1997**, *16*, 689–694.
[25] C. Ruiz-perez, M. Hernandez-Molina, P. Lorenzo-luis, F. Lloret, J. Cano, M. Julve, *Inorg. Chem.* **2000**, *39*, 3845–3852.
[26] a) Z.-N. Chen, S.-X. Liu, T. Qiu, Z.-M. Wang, J.-L. Huang, W.-X. Tang, *J. Chem. Soc., Dalton Trans.* **1994**, 2989–2993; b) C. B. Ma, C. N. Chen, Q. T. Liu, F. Chen, D. Z. Liao, L. C. Li, L. C. Sun, *Eur. J. Inorg. Chem.* **2003**, 2872–2879.
[27] a) M. Wesolek, D. Meyer, J. A. Osborn, A. Decian, J. Fischer, A. Derory, P. Legoll, M. Drillon, *Angew. Chem. Int. Ed. Engl.* **1994**, *33*, 1592–1594; b) S. L. Lambert, D. N. Hendrickson, *Inorg. Chem.* **1979**, *18*, 2683–2686; c) H. Chang, S. K. Larsen, P. D. W. Boyd, C. G. Pierpont, D. N. Hendrickson, *J. Am. Chem. Soc.* **1988**, *110*, 4565–4576; d) K. K. Nanda, L. K. Thompson, J. N. Bridson, K. Nag, *J. Chem. Soc., Chem. Commun.* **1994**, 1337–1338.
[28] M. E. Fisher, *Am. J. Phys.* **1964**, *32*, 343–346.
[29] C. J. O'Connor, *Prog. Inorg. Chem.* **1982**, *29*, 203–283.
[30] G. W. Sheldrick, *SADABS*, Program for Empirical Absorption Correction of Area Detector Data, University of Göttingen, **1996**.
[31] G. W. Sheldrick, *SHELXS 97*, Program for Crystal Structure Solution, University of Göttingen, **1997**.
[32] G. W. Sheldrick, *SHELXL 97*, Program for Crystal Structure Refinement, University of Göttingen, **1997**.

Received: November 4, 2005
Published Online: February 24, 2006

